JOURNAL OF MATERIALS SCIENCE 27 (1992) 1023–1035

Synthesis and characterization of primary alumina, titania and binary membranes

V. T. ZASPALIS, W. VAN PRAAG, K. KEIZER, J. R. H. ROSS, A. J. BURGGRAAF
Faculty of Chemical Technology, Laboratory for Inorganic Chemistry, University of Twente, Materials Science and Catalysis, PO Box 217, 7500 AE Enschede, The Netherlands

The synthesis and characterization of supported and non-supported membranes of γ-Al_2O_3, TiO_2 and their binary combinations are described. Non-supported γ-Al_2O_3 and TiO_2 membranes were prepared from colloidal dispersions (sols) of boehmite and titania, respectively. Stable binary sols were also prepared by mixing boehmite and titania sols under appropriate pH conditions, and these were used to prepare binary (γ-Al_2O_3/TiO_2) membranes. Supported γ-Al_2O_3, TiO_2 and binary membranes were made by the slip-casting process using the same sols. The membrane layers had, after calcination, a thickness of 3–6 μm depending on the dipping conditions, and an average pore diameter of ~3–4 nm with a narrow pore-size distribution. The structural transformation of titania from the anatase to the rutile phase was retarded by performing the hydrolysis in the presence of sulphate ions. Polyvinyl alcohol was added to the sols to strengthen the gel network during the drying and calcination process. This resulted in a less critical and more controllable membrane formation process. Multiple dipping (e.g. to repeat the dipping, drying and calcination steps) appeared to be a technique by which (i) defected layers could be repaired; (ii) thick membrane layers could be prepared; and (iii) multilayer membranes consisting of layers of different components could be prepared.

1. Introduction

Membranes can be defined as semi-permeable barriers that prevent intimate contact between two homogeneous phases, but allowing preferential passage of certain species across their structure. On a material basis, membranes can be classified according to Table I.

Membrane applications include separations in the microfiltration (particulate/molecular size of 1000 nm), ultrafiltration (particulate/molecular size up to 100 nm) and reverse osmosis (particulate/molecular size 0.1 to 1 nm) regions (e.g. in treatment of municipal or industrial waste streams, in food processing, water desalination, biomedical processes, metal, textile, paper and chemical industries [1–4]). Recent membrane applications include gas separations [5] and catalytic applications in low-temperature membrane reactors (e.g. enzyme immobilization techniques in bioprocesses [6]) or in high-temperature membrane reactors [e.g. 7–11].

Polymeric membranes have been commercially available for many years and are employed in large-scale operations; they offer significant flexibility and can respond successfully to a wide range of process requirements. However, polymeric membranes 'suffer' from the polymeric properties. Non-aqueous organic solvents, dry atmospheres or high temperatures (above 250 °C) might deteriorate the membrane material sufficiently to cause its collapse and a complete loss of permeability. The use of either high or low pH might cause hydrolysis of the membrane material; this might also be sensitive to attack by enzymes or micro-organisms. These conditions of operation can be covered by the thermally and chemically more stable inorganic membranes, and so the membrane technology application field can be extended significantly.

The potential applications and possibilities of inorganic membranes have recently been extensively reviewed in the literature [12–15]. The thermal stability of these materials allows them to be used either directly as catalysts or in combination with catalysts in high-temperature membrane reactor processes. Although the fundamental idea already existed [16], evaluations of the various aspects of such a concept have been recently published [17], accompanied by theoretical [7–9] or experimental [10, 11, 18–20] data.

Two categories of inorganic membrane can be distinguished on a structural basis: porous and non-porous. Non-porous inorganic membranes, metallic as well as oxidic, exhibit high selectivities towards permeating species; their permeabilities are however quite low, mainly as a consequence of the transport mechanism. In most cases, this is an activated solution–diffusion process [21, 22]. The stability of metallic membranes is questionable; for example, after repeated adsorption/desorption cycles, or after use under steam-containing atmospheres or at elevated

0022–2461

TABLE I Membrane classification on material basis

1. Organic polymers
2. Inorganic polymers
3. Organic–inorganic polymers
4. Other inorganic materials
(a) Ceramics
(b) Glasses
(c) Metals

TABLE II Synthesis methods for porous inorganic membranes

1. Separation/leaching [53]
2. Anodic oxidation [54]
3. Pyrolysis [55]
4. Thin-film deposition [56]
5. Track-etching [57]

temperatures (above 300 °C) where degradation of the metallic structure may occur. Porous inorganic membranes exhibit higher permeabilities but lower selectivities than non-porous membranes. Recent research on this point, focused on specific gas transport mechanisms, promises considerable improvements [23, 24].

Increased use of inorganic membranes has led to improved methods of preparation [25–27]. Porous inorganic membranes can be prepared in various ways, those depending on the materials used and on the required structural characteristics (e.g. pore size, porosity and membrane thickness). The most common and widely documented methods for the synthesis of porous inorganic membranes are listed in Table II.

It has been shown in the last decade that it is possible to prepare ultrafine-grained ceramics with high density when a ceramic compact consisting essentially of very fine crystallites, having small pores and a very narrow pore-size distribution, is used as the starting material for the sintering process [28]. This narrow pore-size distribution is obtained as a result of regular particle stacking achieved from sols instead of powders. The sol–gel process is thus an established method for producing uniform nanometre-size particles as precursors for the synthesis of membranes to be used as ultrafiltration, hyperfiltration and gas separation membranes. In the sol–gel process for the production of metal oxides, the colloidal sols can be prepared by a number of different routes such as polycondensation of metal salts to form oxides [29], reactions of aqueous solutions of metal salts with organic reagents [30], or hydrolysis and polycondensation of metal alkoxides [31, 32]. The last route is the most versatile and has been investigated extensively [33]. The process of hydrolysis and polycondensation allows the different precursors to be mixed on a molecular level (to yield multicomponent ceramics). The method can be also used to produce high-purity and ultrafine particles.

The synthesis of membrane materials via the sol–gel route (hydrolysis and polycondensation of alkoxide precursors) and the characterization of thin ceramic membrane layers of γ-Al_2O_3 and TiO_2 with small pores (mean pore radius of ~ 2 nm) and with narrow pore-size distributions are described.

2. Materials and characterization methods

All the chemicals used were obtained from Merck (analytical grade). Distilled water was used as solvent in all cases. X-ray diffraction (XRD) studies were carried out with a Philips PW 1370 X-ray diffractometer with Ni-filtered Cu$K\alpha$ radiation. Pore size measurements were performed with a Carlo Elba mercury porosimeter (200 series) and surface-area measurements (BET method using N_2 at 77 K) were made with either a Carlo Elba Sorptomatic (type 1800) or a Micromeretics (ASAP 2400) system. All three systems were computerized. Jeol JSM-35CF with energy dispersive analysers of X-rays (type EDAX or KEVEX) and Jeol-200CX electron microscopes were used for scanning (SEM) and transmission (TEM) electron microscopy studies, respectively. A DuPont 951 thermogravimetric analyser was used for thermogravimetric analysis (TGA) in air. De-agglomeration of titania colloidal dispersions was performed in a Branson 2200 ultrasonic bath. A Heraeus Vötsch climate chamber was used for the drying of the ceramic membrane layers. Particle sizes in the sol phase were examined by the dynamic laser-scattering technique at 25 °C using a Malver Autosizer 2c unit. Gas and water permeability measurements were performed according to van Vuren *et al.* [34].

3. Experimental procedure

Ceramic membranes of γ-Al_2O_3, TiO_2 and their binary combinations were prepared by a process in which stable sols of boehmite, titania or a binary mixture were successively slip-cast onto a porous substrate, gelled and processed (i.e. dried and calcined). In some cases non-supported membranes were also synthesized.

3.1. Sol preparation

The synthesis of boehmite (γ-AlOOH) sols as well as microstructural investigations of the products of dehydration of the γ-AlOOH sol have been described elsewhere [31]. (The term 'sol dehydration products' is equivalent to the term ' non-supported membranes' or 'thin films'. Non-supported membranes were prepared from sols via solvent (water) evaporation.) Titania colloidal sols were prepared by hydrolysis of titanium tetra-isopropoxide [$(i\text{-}C_3H_7O)_4Ti$]. A volume of 400 cm^3 of water per mole of alkoxide was used to bring about hydrolysis. A solution of titanium tetra-isopropoxide in isopropanol (0.45 mol dm^{-3}) was added dropwise to a solution of water in isopropanol (4.5 mol dm^{-3}) while stirring at high speed. In a standard laboratory experiment, 0.1 mol of alkoxide was hydrolysed with 40 cm^3 water. Hydrolysis was carried out at room temperature and preferably in a water-free atmosphere, which was realized by supplying dry nitrogen above the hydrolysis vessel. The resultant

white precipitate of titanium hydroxide was filtered and subsequently washed with water to remove the alcohol. The product was then diluted in water to a metal (Ti^{4+}) concentration of about 0.2–0.3 mol dm^{-3}, and peptized with nitric acid, added to achieve a ratio of H^+/Ti^{4+} of 0.5. Peptization proceeded overnight at about 70 °C while refluxing. The result was a stable semi-opaque titania dispersion. Further peptization was performed by immersing the dispersion in an ultrasonic bath. Small portions of the dispersion (~ 20 ml) were poured in beaker glasses and subsequently held for 20 min in a water bath subjected to ultrasonic energy. Sound waves from the transducer radiated through the liquid in the bath in which the beaker glasses with sol were placed, at ultrasonic frequencies and with a power of 60 W. A clear blue stable titania sol was the final product. Titania sols so produced had a final metal concentration of 0.2 mol dm^{-3}. Lower concentrations could be achieved simply by dilution with water, and higher concentrations by evaporation at 40–50 °C under vacuum, in a rotavapor.

Stable binary sols were prepared by physical mixing of the individual titania and boehmite sols at pH values lower than 5 (preferably at pH ~ 2).

3.2. Formation of membranes or thin films

Membrane layers of γ-Al_2O_3, TiO_2 and of γ-Al_2O_3/TiO_2 were made either in a free non-supported form, or supported on top of α-Al_2O_3 substrates. The non-supported films were used for characterization as there was no interference with the support. Supported membranes have better mechanical stability and can be mounted in cells for process performance measurements (e.g. catalytic activity or gas separation). Extrapolation of the structural results of non-supported films to supported membranes requires that the two are structurally similar. Results from gas permeability and adsorption/desorption measurements on supported and non-supported membranes demonstrated that this was indeed the case.

The supports consisted of flat circular plates of α-alumina with a diameter of 39 mm and a thickness of 2 mm. They were made by a process in which a commercially available powder was pressed at a pressure of ~ 100 MPa, calcined at 1200 °C for ~ 2 h after heating at a rate of 100 °C h^{-1} and subsequently cooling at the same rate. The structural characteristics of the support (determined by mercury porosimetry) are shown in Fig. 1. The support surface was polished and cleaned with water before use.

Non-supported membranes were formed from γ-Al_2O_3, TiO_2 and γ-Al_2O_3/TiO_2 sols by evaporation of the water solvent. Small amounts of sol were poured in polypropylene petri dishes and subsequently allowed to dry at 40 °C and at 60% relative humidity ('free gelation') in a climate chamber in which air at the above conditions was circulated. The thickness of the non-supported membranes (sol dehydration products) prepared in this way and after calcination varied between 50 and 100 μm, depending on the amount of sol used.

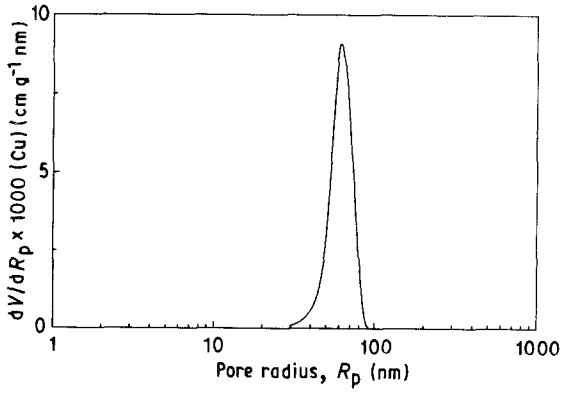

Figure 1 Structural characteristics of support material plot of differential pore volume as a function of pore size.

Supported membranes were formed by bringing the sol into contact with the dry support. The capillary pressure drop thus created by the pores of the support (ΔP_c) forces the dispersion medium into the support, while the particles are concentrated at the surface and gelation occurs ('forced gelation'). A qualitative as well as quantitative description of the so-called dipping (slipcasting) process has been given elsewhere [35]. Fig. 2 shows the supported membrane formation process.

3.3. Membrane processing

The processing of the supported or non-supported membrane layers included drying at 40 °C and 60% relative humidity for 3 h, followed by calcination at 600 °C for 3 h for the alumina membranes and at 450 °C for 3 h for the titania and binary membranes. The drying conditions, as well as the heating and cooling rates, are not of major importance for the non-supported layers. They are, however, very critical for the supported membranes in order to avoid cracking of the top layers. Heating and cooling rates of 10 °C h^{-1} were therefore chosen.

3.4. Introduction of additives

The process for the synthesis of supported membranes as described above did not always lead to continuous and crack-free top layers in the supported membranes. In particular, for the titania membranes and to a lesser extent for the binary and alumina membranes, a considerable number of the supported membranes showed cracks present in the top layer after calcination. The stresses developed during drying and calcination in these cases exceeded the rupture strength of the gel network, and as a result cracks were formed. To avoid this problem, organic additives were added to the dipping solution. The best results were obtained using polyvinyl alcohol (PVA) (mol wt 72 000 Da), in the cases of the alumina and binary membranes and PVA in combination with hydroxypropyl-cellulose (HPC) (mol wt 10^5 Da) in the case of the titania membranes. In addition to improved yield of the synthesis process, the introduction of organic additives appeared also to enable the acceleration of the calcination step from heating and cooling

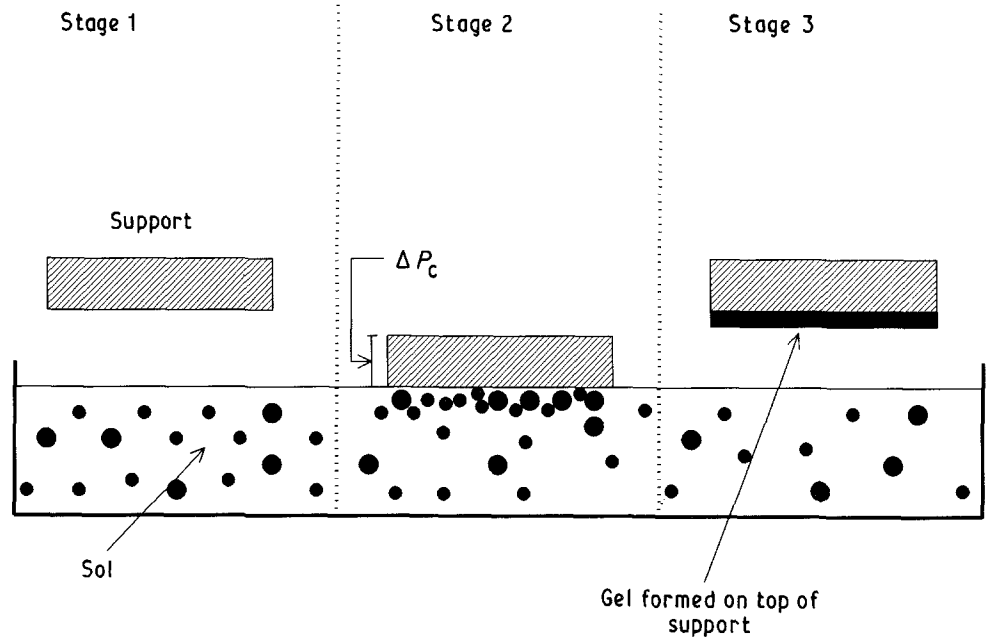

Figure 2 Schematic presentation of the three stages of the dipping process.

rates of 10 °C h^{-1} to heating rates of 60 °C h^{-1} and natural cooling.

An additional problem concerning the synthesis of titania membranes was the phase transformation from the anatase to the rutile structure which is stable at high temperatures. This phase transformation introduces a volume change of 8% which is enough to originate defects in the titania layer. In order to retard this titania phase transformation, at least until the final calcination temperature (450 °C), sulphate ions in the form of sulphuric acid (5 cm^3 H_2SO_4 per mol alkoxide) were introduced in the hydrolysis vessel before the precipitation of titanium hydroxide. The hydrolysis was carried out in the presence of sulphate ions for the synthesis of titania membranes aimed to be used as catalysts in a membrane reactor and at high temperatures. For the synthesis of non-supported titania films or of titania membranes used at room temperature (e.g. characterization by adsorption–desorption, gas or water permeability) the hydrolysis was carried out in the absence of sulphuric acid.

A typical dipping solution for the synthesis of γ-Al_2O_3 supported or non-supported membranes consisted of 30 cm^3 of 1 mol dm^{-3} boehmite sol (prepared according to Leenaars *et al.* [31]) mixed with 20 cm^3 aqueous PVA solution at a concentration of 3.5 g per 100 cm^3. The dipping time was 4 s for a calcined layer thickness of $\sim$ 3 μm.

A typical dipping solution for the synthesis of TiO_2 supported or non-supported membranes consisted of 30 cm^3 of 0.1 mol dm^{-3} titania sol mixed with 10 cm^3 aqueous PVA solution at a concentration 0.1 g per 100 cm^3 and 20 cm^3 aqueous HPC solution at a concentration 0.35 g per 100 cm^3. The dipping time was 4 s for a calcined layer thickness of 1 μm.

A typical dipping solution for the synthesis of binary γ-Al_2O_3/TiO_2 membrane of desired composition was obtained by mixing 20 cm^3 boehmite sol, 1 M, pH < 5, with the appropriate volume of titania sol 0.2 mol dm^{-3}, pH $\sim$ 2, and with the appropriate volume of aqueous PVA solution at a concentration of 0.1 g PVA per 100 cm^3, so that the final PVA content approximated 3 wt. % of the total boehmite and titania phase. The dipping time was 2 s for a calcined membrane thickness of 1–2 μm.

In a standard membrane formation procedure, dipping in the solutions that are described above, drying and calcining were repeated three times. The standard resulting membrane thicknesses were 7–8 μm for γ-Al_2O_3 membranes, and 4–5 μm for TiO_2 and for binary membranes.

3.5. Multiple dipping

The continuity and thus the quality of these supported membranes was tested by gas permeability [34]. This method is very sensitive to any pinholes or defects present in the top layer, even at low concentrations. It may happen that during the dipping procedure, due to the presence of irregularities on the support surface or for other reasons, e.g. the presence of microscopic air bubbles in the sol, pinholes (areas where layer formation did not take place) are formed, even though the membrane layer does not crack. This type of defect could be repaired by repeating the dipping, drying and calcination steps, as described previously, two or three times.

Another reason for multiple dipping was the increase in membrane thickness. For catalytically active membranes, membrane thickness is directly related to the residence time of the reactants in the top layer of the membrane. The number of dipping times and the resulting membrane top layer thicknesses in a standard synthesis have been mentioned above.

4. Results and discussion

4.1. Sol preparation

The preparation of boehmite sols has been discussed elsewhere [31]. For the preparation of titania sols,

titanium alkoxide (tetra-isopropoxide) was used as the metal precursor as the other commonly used metal precurosr, $TiCl_4$ [36], requires special handling and working conditions and gives hydrolysis rates which are difficult to control. The alkoxide and water were both diluted in excess of alcohol to ensure control and uniformity of hydrolysis rates. For the same reason, precipitation was carried out at room temperature. Hydrolysis experiments using $TiCl_4$ as metal precursor or without diluting the reactants in isopropanol or at higher temperatures (e.g. 80 °C) resulted in highly agglomerated unpeptizable products. The hydrolysis (precipitation) reaction of titanium tetra-isopropoxide in aqueous isopropanol can be described by the following equation

$$Ti(OC_3H_7)_4 + xH_2O \rightarrow Ti(OH)_x(OC_3H_7)_{4-x} + xC_3H_7OH \quad (1)$$

where for $x = 4$ (excess of water) the result is a colloidal sol.

The effects of the hydrolytic polycondensation parameters during the hydrolysis of titanium alkoxides have been discussed in the literature [37, 38]. As discussed below, sulphate ions in the form of sulphuric acid were added in the hydrolysis vessel before precipitation in order to stabilize the anatase structure of titania. The hydrolysis in these cases was carried out in the presence of low concentrations of sulphate ions. This may influence the hydrolysis and polycondensation of titanium isopropoxide, giving rise to different particle sizes and subsequently different packing and structural properties of the membranes than those expected if no sulphate ions were present during the hydrolysis. As is shown in Table III the resulting structural differences were quite small.

The washing step after hydrolysis was critical for the preparation of titania sols and had to be carried out very rapidly. The titanium hydroxide precipitate was filtered and subsequently washed on the filter from the rest of the alcohol with water. This stage must not last too long and the precipitate must not be allowed to dry on the filter. Long washing periods appeared to give rise to the formation of agglomerates, making the subsequent peptization step very difficult. It is known that titanium isopropoxide exhibits higher hydrolysis rates than aluminium butoxide [33, 37]. On the other hand, elimination of the washing step did not result in peptizable sols. The presence of the alcohol inhibited the peptization function of the acid.

The peptization of the titanium hydroxide product proceeded with acid. In this way the existing agglomerates were dispersed and a positively charged (H^+) layer on each individual particle (or possibly around a small group of particles) was created. A stable fine colloidal dispersion was thus obtained which was suitable as starting material for the synthesis of well defined membrane structures. The peptization process can be written as

$$nTi(OH)_4 + xH^+A^- \rightarrow [Ti(OH)_4]_nxH^+ + xA^- \quad (2)$$

The most important parameters were the nature of the peptizing agent, the amount of peptizing agent (resultant pH), peptization temperature and peptization time. Peptization did not take place at low temperatures. The peptization process was not carried out at constant pH: it is thus possible that during the addition of acid to the hydroxide precipitate solution, and during the peptization (stabilization) process, pH variations occur until the final value. Peptization occurred at sufficient rate at temperatures of about 70 °C. The effect of the nature and amount of peptizing agent is shown in Table IV. The pH shown in Table IV is the final pH of the sol, when the peptization process was complete. As can be seen from this Table IV, peptization of titania sol did not occur at H^+/Ti^{4+} ratios lower than 0.5, or at a final pH higher than ~ 1.5. Sulphuric acid was not a suitable peptizing agent. Probably in this case the zeta potential of the particles was too low due to the higher charge of the counter ions (SO_4^{2-}). From BET measurements on sol (peptized with HNO_3, $H^+/Ti^{4+} = 0.5$) dehydration products (non-supported membranes) shown in Fig. 3, it appears that the peptization process with HNO_3 was complete after about 20 h.

The product after peptization was a stable white colloidal dispersion, which was still not transparent due to the retention of a large number of relatively large agglomerates. These were however soft agglomerates which can be broken up with the help of

TABLE III Structural data for stabilized and non-stabilized titania membranes calcined for 3 h at 450 °C

Sample	Pore diameter (nm)	BET surface ($m^2 g^{-1}$)	Porosity (%)
Without SO_4^{2-}	4.5	50.6	25
With SO_4^{2-}	4	77	30

TABLE IV Results for the peptization of titania sols with different acids and at two different pH values

Type of acid	pH (final)	H^+/Ti^{4+}	Peptization
HNO_3	1.5	0.5	Yes
HNO_3	3	0.35	No
HCl	1.5	0.5	Yes
H_2SO_4	1.5	0.5	No

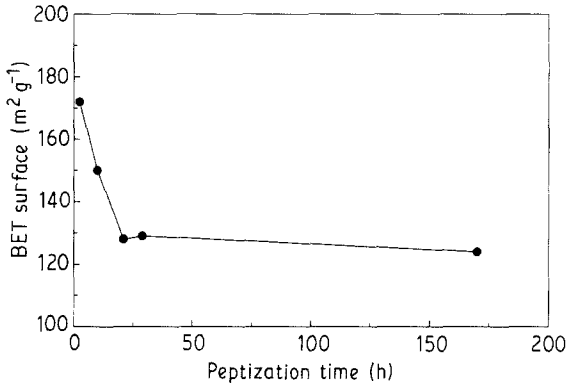

Figure 3 BET surface area of titania sol dehydration products peptized with nitric acid ($H^+/Ti^{4+} = 0.5$) as a function of peptization time at 70 °C.

ultrasonic energy. By immersing the sol in an ultrasonic bath, the peptization process could be completed and a blue semi-opaque colloidal dispersion was the final product. The average particle size measured by dynamic laser scattering is shown in Table V for titania sols peptized under different conditions. For comparison, data from measurements with alumina sols are also presented. As can be seen from samples 1–3, the peptization process was not complete after the treatment with acid. The residual agglomerates could, however, be broken down with the use of ultrasonic energy. From samples 3 and 4 of Table V it can be concluded that a certain degree of ageing occurred in the sol. A comparison of samples 2 and 5, and of 3 and 6 (Table V) indicates that the resultant average particle size was also a function of the peptization agent used (a similar result was also observed with boehmite sols [35]). The particle-size distributions of samples 2 and 3 (Table V) are shown in Fig. 4. As can be seen from Fig. 4, the use of ultrasonic energy resulted in a narrow particle size distribution as well as a smaller particle size. Small particle sizes and uniform distributions in the sol state are desirable properties for the formation (by the process shown in Fig. 2) of well defined membrane top layers which, after calcination, have small pores and uniform pore-size distribution.

During the mechanical mixing of titania and alumina sols, flocculation due to destabilization might occur. The surface charge of the particles has to be of the same sign. In the case of peptization with acid (positively charged particles) flocculation will happen if the pH of the binary mixtures exceeds the isoelectric point of one of the stabilized components. The isoelectric point of alumina was determined to be $\sim$ 6–7, while that point of titania was $\sim$ 5. In order to avoid destabilization of the resultant sol, the pH of the alumina sol was brought below 5 before mixing, by the addition of nitric acid. Stable binary sols could be prepared under these conditions, which were suitable starting materials for the formation of binary membranes [39].

4.2. Non-supported membranes

In order to establish the calcination conditions and the structure of the calcined supported membranes, microstructural investigations were carried out with non-supported membranes; these were the dehydration products of the above described sols. A typical TGA curve for titania unsupported membranes after drying is shown in Fig. 5. The same type of curves were also obtained for non-supported binary and alumina membranes. As can be seen from Fig. 5, initially and until about 130–140 °C, water condensate in the pores and water adsorbed on the surface of the pores evaporates. From 150–450 °C, crystallization of $Ti(OH)_4$ to TiO_2 takes place. At 450 °C, the transformation of the hydroxide to the oxide was completed. At 350 °C, the total weight loss was 90% of the final value. This is in agreement with the literature [40]. In Table VI, the structural characteristics of alumina, titania and binary non-supported membranes calcined at different temperatures are given. In all cases the pore size distribution was sharp around the average value shown in Table VI. As can be seen, the structure of titania maintained its mesoporous properties until a temperature of about 450 °C. Above this temperature (which was also established to be the maximum calcination temperature) destruction of the microstructure occurred, mainly due to sintering and secondly due to phase transformation, as discussed below. It is surprising that for binary non-supported membranes (even those containing 65 wt % titania which corresponds to 66 vol % titania) the structure approximated the large surface areas and porosity of

TABLE V Laser scattering measurements on titania and alumina sols

Sample No.	Characteristics	Particle size* (nm)
1	Ti-sol (not peptized)	> 350
2	Ti-sol (peptized with HNO_3)	175
3	Ti-sol (peptized with HNO_3, subjected to ultrasonic energy)	30
4	As ample 3 (aged for 2 months)	44.5
5	Ti-sol (peptized with HCl)	222
6	Ti-sol (peptized with HCl subjected to ultrasonic energy)	50
7	Al-sol (prepared according to [31])	80

* Average value of three measurements.

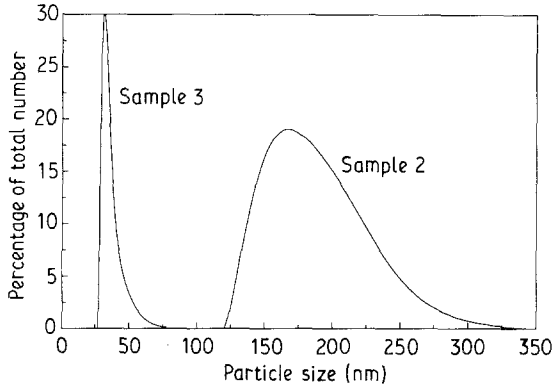

Figure 4 Particle-size distributions of sol samples 2 and 3 (Table V).

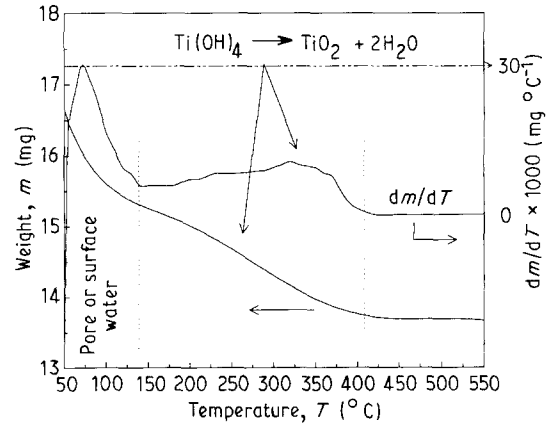

Figure 5 TGA curves for titania non-supported membranes.

TABLE VI Structural properties of non-supported membranes

Sample	Pore diameter (nm)		Porosity (%)	BET surface ($m^2 g^{-1}$)
	Pore model 1*	Pore model 2†		
TiO_2 (3 h at 300 °C)	2.54	3.78	30	119
TiO_2 (100 h at 300 °C)	2.82	4.26	29	73
TiO_2 (3 h at 400 °C)	2.98	4.56	30	85
TiO_2 (3 h at 450 °C)	3.0	4.6	22	80
TiO_2 (3 h at 500 °C)	4.86	7.96	19	31
TiO_2 (3 h at 600°C)	11.74	20.6	21	10
γ-Al_2O_3 (3 h at 450 °C)	2.7	4.0	53	302
γ-Al_2O_3 (3 h at 600 °C)	3.0	—	47	202
γ-Al_2O_3/TiO_2 (70/30 wt %) (3 h at 450 °C)	2.5	3.7	48	260
γ-Al_2O_3/TiO_2 (35/65 wt %) (3 h at 450 °C)	2.5	3.8	38	220

* Pore diameters determined assuming slit-shaped pores.
† Pore sizes determined assuming cylindrically shaped pores.

alumina membranes. A possible explanation is that the final calcined, non-supported membrane consists of a dominating alumina structure similar to that proposed by Leenaars *et al.* [31], with titania particles incorporated within the main alumina framework.

In Table VI, pore diameter values are given based on either slit-shaped or cylindrical pore models. The slit-shaped pore model better approximates the γ-Al_2O_3 structure; the cylindrical pore model the TiO_2 structure. TEM studies for titania indicate that the particles had a roughly spherical shape.

The structure development of non-supported titania membranes during the calcination step is shown in Fig. 6. As can be seen, significant structural changes take place during the calcination of the titania layers. For supported membrane layers these structural changes must not lead to cracks and defects in the membrane layers. For this reason, slow heating rates (10 °C h^{-1}) must be used during the calcination of supported titania membranes.

An important aspect associated with the structural development of titania membranes is the phase transformation occurring at higher temperatures. Titania layers were initially XRD-amorphous and at temperatures up to 300 °C were well crystallized in the anatase structure. It was observed that after 3 h at 400 °C (and after 100 h also at 300 °C) a significant percentage of the high temperature stable rutile structure was present. These transformation temperatures are quite low compared to those reported in the literature [40]. This structural transformation involves a collapse from the relatively open anatase structure with a cell volume of 0.068 nm^3 to rutile with a cell volume of 0.0624 nm^3, a volume change of about 8% [41]. When the titania membrane layers are in supported form, this volume change introduces extra stresses during sintering, and this might destroy the continuity of the membrane. For this reason the phase transformation has to be avoided, at least until the final calcination temperature. Table VI shows that after calcination at 300 °C for 3 h the pore diameter was 3.78 nm, while after 100 h at the same temperature the pore diameter was 4.26 nm (in both case calculated assuming cylindrically shaped pores). The stabilization of the anatase structure has been studied extensively in the literature [42–46]. It has been suggested that oxygen vacancies act as nucleation sites for the rutile phase. The nucleation of rutile starts at the surface and propagates to the bulk of the material. The stabilization of anatase or the retardation of the transformation rate then requires a reduction of the number of surface oxygen vacancy sites of anatase. For this reason, sulphate ions in the form of sulphuric acid were added to the hydrolysis solution before the precipitation. In Table VII, the structure of titania non-supported membranes prepared from sols in the presence and in the absence of sulphate ions is shown. As it can be seen from Table VII, sulphuric ions could indeed retard the transformation of anatase to rutile at least until the maximum calcination temperature. Comparison of adsorption–desorption results between stabilized and non-stabilized samples indicates that under the same calcination conditions, larger surface areas and smaller pores are obtained if the hydrolysis is carried out in the presence of sulphate ions, as shown in Table III.

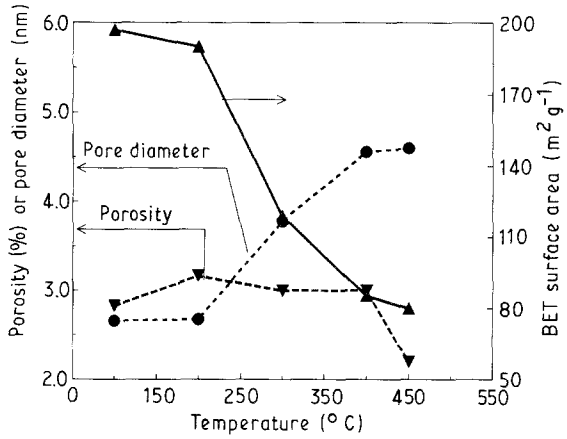

Figure 6 Structural development of titania membranes during calcination.

4.3. The introduction of organic additives

It has been mentioned that the membrane formation

TABLE VII X-ray diffraction results for non-supported titania membranes

Sample characteristics	Calcination temperature (°C)	Time at final temperature (h)	Anatase (%)	Rutile (%)
Hydrolysis carried out in absence of sulphuric ions	Not calcined	–	am./an.*	–
	300	3	100†	–
	300	100	91‡	9
	400	3	87	13
	450	3	< 87¶	–
	500	3	40	60
	600	3	–	100
Hydrolysis carried out in presence of Sulphuric ions	Not calcined	–	am./an.	–
	450	3	100	–
	600	3	100	–

* Mainly amorphous with crystallization tendencies to anatase
† Guirnier camera experiments showed that initially also some brookite is formed
‡ Quantitative approximation of the phase composition is made by correlating the relative intensities of the (110) line of rutile and the (101) line of anatase [54]
¶ For this sample the background level did not allow more accurate determination

process does not always lead to top layers without defects or pinholes. To make the synthesis less critical, organic additives were introduced to the sol before the formation of supported membranes by the slip-casting process. Polyvinyl alcohol was introduced to the alumina and to the binary sol; the amounts have been described previously. Polyvinyl alcohol in combination with hydroxy-propyl cellulose was introduced to the titania sol. Additions of polyvinyl alcohol to titania sols at amounts higher than 1–2 wt % of titania resulted in destabilization and flocculation of the sols. This is due to interaction which takes place between titania and PVA. In the presence of hydroxyl-propyl cellulose, this interaction does not take place and the stability of the titania dispersion is not disturbed. Consequently, higher amounts of PVA can be added to titania sols. The amounts of organic additives given previously are the minimum amounts necessary to achieve a layer which, after treatment, will remain crack-free with sufficient reproducibility.

The exact mechanism by which the organic additives (binders) work is not known. Various theories concerning the role of the organic additives are reviewed by Zarzycki [47]. A possible mechanism might be the strengthening of the gel network by neck growth. Another possibility is the elimination of differential stresses originating from asymmetrical and non-uniform pore structures [48].

An important point associated with the introduction of organic additives in the sols is that the binder has to be burned out before the final calcination temperature, without causing structural defects and irregularities. TGA measurements of pure PVA and HPC showed that they indeed decompose at temperatures below 450 °C. A special type of PVA (Fluka Chemie) and of HPC (Aldrich Chemical Co. Inc.) which did not leave ash or other residues after burning out were used. Fig. 7 shows a TGA curve for a non-supported titania membrane prepared with the use of organic additives. It can be seen that the decomposition and burn-out of the PVA and HPC started at about 250 °C and was complete at the final calcination

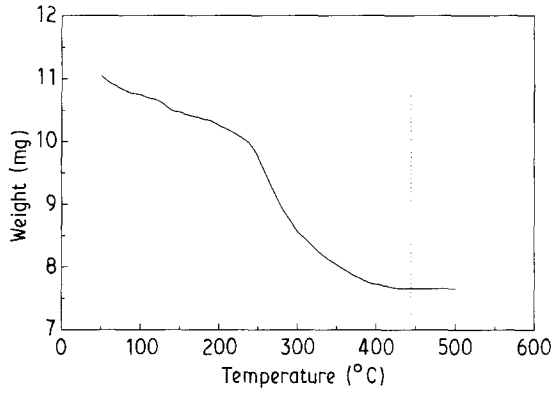

Figure 7 TGA curve of a titania membrane prepared with the use of organic additives.

temperature (450 °C). The pronounced weight loss indicated by the curve of Fig. 7, compared with the weight loss of the TGA curve of Fig. 5 which corresponds to titania thin films without additives, also indicates the burn-out of the organic additives in the temperature region between 250 and 400 °C.

Figs 8–10 show nitrogen adsorption/desorption curves and the corresponding pore-size distributions for titania membranes prepared under different conditions. All samples were prepared by carrying out hydrolysis in the absence of SO_4^{2-} ions. Fig. 8 gives the results for a sample prepared without any addition of organic additives; Fig. 9 for a sample prepared according to the standard procedure (see above); and Fig. 10 for a sample prepared according to the standard procedure, except that a higher molecular weight HPC was used. Comparing Figs 8 and 9, it can be concluded that the introduction of organic additives did not result in significant structural changes. The microporous properties of the membranes were retained and, as discussed in a subsequent section, the Knudsen diffusion characteristics were also unchanged. The desorption curve of Fig. 9 however, is less steep than that of Fig. 8, indicating that the introduction of additives resulted in a somewhat

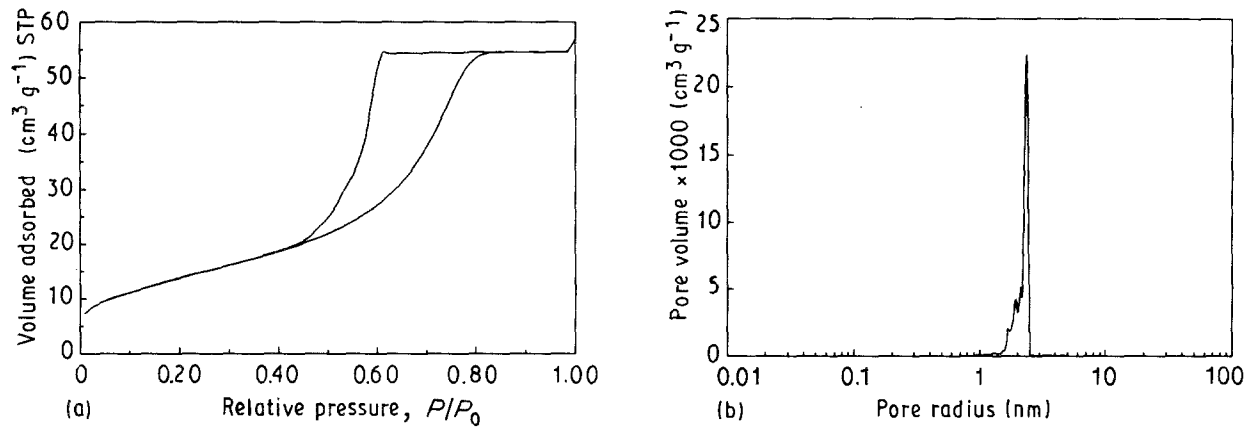

Figure 8 (a) Adsorption isotherms and (b) pore-size distribution for titania layers prepared without the use of organic additives.

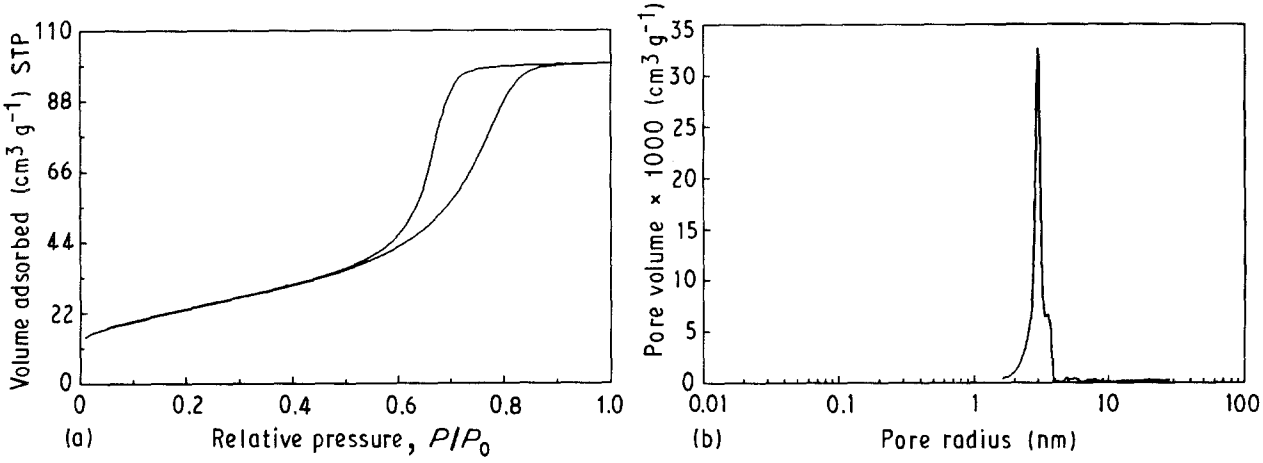

Figure 9 (a) Adsorption isotherms and (b) pore-size distribution for titania layers prepared with the use of organic additives (HPC molar mass 10^5 g).

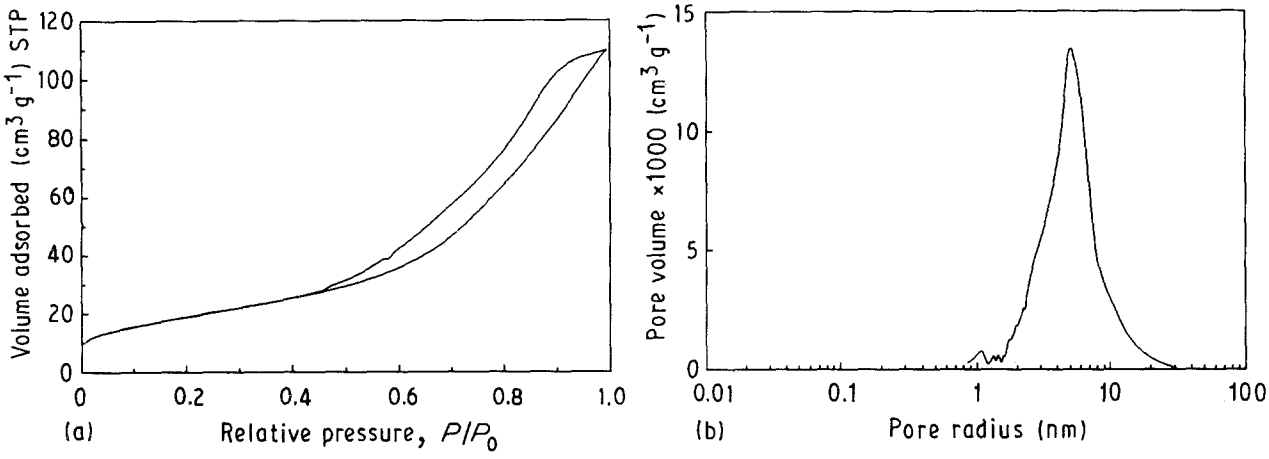

Figure 10 (a) Adsorption isotherms and (b) pore-size distribution for titania layers prepared with the use of organic additives (HPC molar mass 10^6 g).

broader pore-size distribution. The situation is different for the sample shown in Fig. 10. The introduction of HPC with a higher molecular weight than that shown in Fig. 9 resulted in a much broader pore-size distribution and a larger pore size. Membranes with structural properties corresponding to Fig. 10 are, however, suitable for applications where the flux through the membrane is of greater importance than the homogeneity of the structure. The introduction of binders had similar effects on the microstructure of alumina membranes [49].

4.4. Membrane formation and processing

The formation of supported membranes from dipping solutions with the characteristics given above is presented schematically in Fig. 2. It proceeds by the slip-casting mechanism described elsewhere [31]. The influence on the membrane formation process of the

most important parameters (such as sol concentration, viscosity and particle size, dipping time and support pore size) is also described [31]. It is of major importance that the formation of a layer on top of a support proceeds via the slip-casting mechanism and not via a film-coating mechanism. The slip-casting mechanism exploits the capillary pressure exerted by the pores of the support which pulls the sol particles tightly onto the surface. This has the advantage that a homogenized structure can already be achieved during layer formation, and this will lead to uniform microporous structures after processing. Another important advantage of the slip-casting process is that it leads to excellent adherence between top layer and support, a property that makes the membranes suitable for applications in which high back pressures are exerted on the top layer. Top layers do not peel off, e.g. during back-flushing or under pressure differences. The equation which governs the slipcasting mechanism is

$$L_g = \left(\frac{C_g t}{n}\right)^{\frac{1}{2}} + K_s \qquad (3)$$

where L_g is the layer thickness after calcination; C_g is a constant which depends on the structural properties of the gel layer; n is the effective viscosity of the liquid (for water this is $\sim 10^{-3}$ N s m^{-2}); t is the dipping time; and K_s is the thickness of the film adhered to the layer which is formed at $t = 0$ by the film-coating process. It is determined by viscosity effects, and can be determined experimentally by using dense supports. The calcined layer thickness as a function of the square root of the dipping time is shown in Fig. 11 for alumina membranes prepared with and without organic additives (PVA) and for titania membranes prepared with organic additives (HPC and PVA). All lines shown in Fig. 11 correspond to the first dipping procedure with a clean support surface. As can be seen, the slip-casting mechanism was also maintained in the presence of organic additives. It was observed, however, that the line in the presence of organic additives (line 2 of Fig. 11) had a smaller slope compared to that for the line in the absence of organic additives (line 1 of Fig. 11). The somewhat higher intersect, which is too small to be shown clearly in the figure, can be explained by the higher viscosity of the dipping solution in the presence of organic additives. The lower slope is a result of slower slip-casting rate, either because of the higher viscosity or because of the lower surface tension of the liquid in the presence of organic additives. Lower surface tension results in lower capillary pressures and thus in lower slip-casting rates. In all cases, K_s (Equation 1) is of the order of 0.5–1 μm. The value of C_g for titania and alumina (without organic additives) is 5–7.5 10^{-5} N, which means that a total layer thickness of about 10 μm can be achieved after 10 s. For alumina with organic additives, this layer thickness is 2–4 times smaller (C_g, 4–16 times smaller). Line 3 of Fig. 11 shows the results for titania membranes formed from titania sol into which organic additives (PVA + HPC) have been introduced. The adhered layer which was formed by the film-coating process (the layer thickness at $t = 0$) was in this case lower than that of alumina membranes (with or without organic additives) and the layer formation rate (slope of line 3) was larger than that for alumina with organic additives. This implies a smaller viscosity, and the possibility that by adjusting the viscosity thinner layers can be prepared from titania sols rather than from alumina sols.

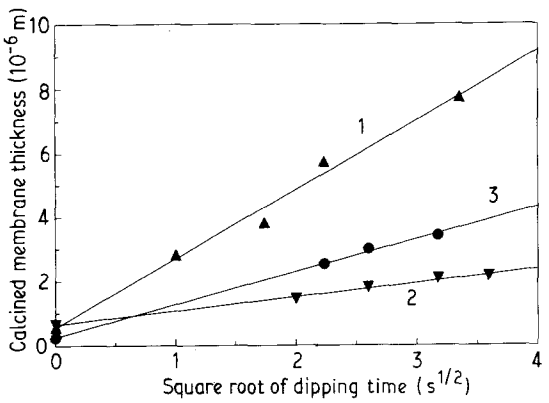

Figure 11 Calcined top-layer thickness as a function of dipping time. ▲, alumina [35]; ▼, alumina + organic additives; ●, titania + organic additives.

Besides careful selection of the processing conditions (drying and calcination), successful membrane formation also requires an optimization of the membrane formation process parameters (support characteristics, dipping time, etc.). The sensitivity of the system to process parameters increases in the range alumina–binary system–titania. This seems to be directly related to the particle shapes and structures of the membrane layer. A model of the alumina involving a card-packed structure with slit-shaped pores, as discussed elsewhere [31] allows stress relaxation in the direction parallel to the membrane surface. Such a relaxation mechanism cannot easily take place with the spherically shaped titania particles. This explains the fact that higher heating rates can be used during the calcination of alumina membranes (60 °C h^{-1}) while the heating and cooling rates must remain slow (10 °C h^{-1}) for titania and binary membranes. Current research is being carried out to prove this [50].

The maximum allowable membrane thickness formed by one dipping procedure also depends on the material used. For alumina membranes, layers with thicknesses of $\sim$ 3–4 μm after calcination could be prepared by one dipping procedure. For titania and binary membranes, the maximum layer thickness per dipping procedure was limited to 1–2 μm. Thicker layers cannot withstand the stresses that develop in the structure during drying and calcination, and will result in defected and cracked membranes, as shown in Fig. 12. This phenomenon might be partially explained by the thin-layer stress-development theory [51, 52]. This theory suggests that the elastic energy released by cracking a thin film is too small to balance the energy required to form a crack. This theory, however, does not directly explain the experimentally observed dependencies of the critical thickness on parameters such as the addition of organic additives or the quality of the support surface.

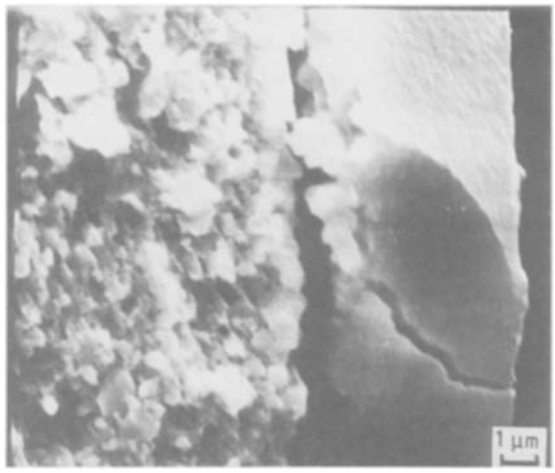

Figure 12 SEM photo of a supported membrane showing cracks after calcination.

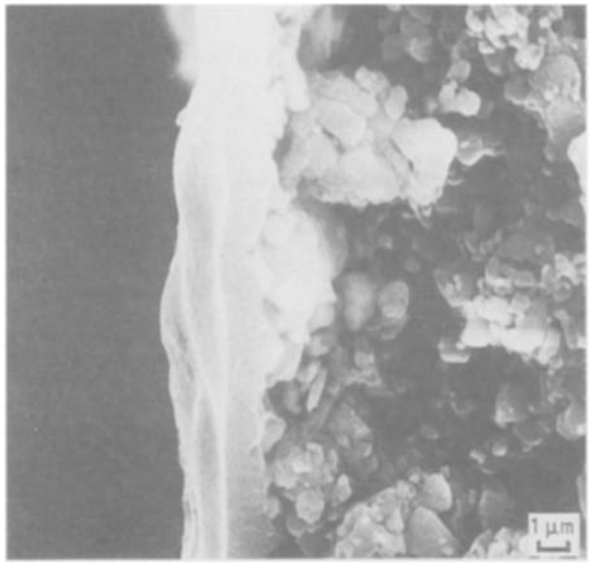

Figure 13 SEM photo showing the transfer of support surface irregularities to the membrane layer surface.

Another very important parameter for the synthesis of supported membranes is the quality of the surface on top of which the membrane is formed. Thin membrane layers follow the irregularities of the substrate surface, as demonstrated in Fig. 13. Rough support surfaces will transfer the roughness to the membrane layers. This is an extra stress-generation factor which might promote the nucleation of cracks and result in defective membranes. Therefore the supports have to be polished thoroughly before use. This also explains experimental observations on titania membranes which could be formed more easily and even without the addition of organic additives on top of previously formed (and calcined) alumina membranes. The surface of an alumina membrane (which now acts as support for the successive deposition of a titania layer) has a much lower roughness than the surface of an α-alumina support.

In order to be used for applications, the supported membranes must not only be crack-free and defect-free under the microscope, but must exhibit certain

TABLE VIII Tortuosities for alumina and titania membranes

Membrane type*	Tortuosity (from helium perm.)	Tortuosity (from water perm.)
γ-Al_2O_3 (600 °C) (with org. add.)	4.5	5.4
γ-Al_2O_3 (800 °C) (no org. add. [50])	–	5.1
TiO_2 (450 °C) (with org. add.)	2.9	3.3

* Final calcination temperature in parentheses.

microporous properties concerning the transport of gases or liquids through their structure. The existence of defects and macropores can be detected very sensitively by gas permeability measurements. Water permeability measurements can provide useful structural information concerning the membrane layers. Helium and water permeability measurements are shown in Fig. 14 for a titania membrane with a thickness of 4 µm. As can be seen from this figure, both types of permeability exhibited the theoretically predicted behaviour as described previously [34]. The helium permeability of the top layer was pressure-independent, indicating that a defect- and imperfection-free membrane top layer has been formed in which only Knudsen diffusion takes place. The water permeability showed linear behaviour with the pressure difference, in agreement with the Kozeny–Carman equation [35]. Useful information can be extracted concerning the structure of the supported membranes from both gas and water permeability measurements. The tortuosities of both alumina and titania membranes are given in Table VIII. These were calculated from gas and water permeability measurements. From Table VIII it can be concluded, in agreement with the previous discussion, that the introduction of organic additives did not cause significant structural changes. The tortuosity values determined by helium and by water permeabilities were in good agreement. The tortuosity of titania membranes was lower than the tortuosity of alumina membranes. This can be explained if the differences in particle shapes and structure of both membranes are taken into account. The card-packed structure of the alumina plate-shaped crystallites has a higher tortuosity than the titania structure. The latter consists of more or less spherically shaped crystallites. The tortuosity values were in agreement with the expectations from these models.

In a number of cases, the multiple dipping technique is useful. In cases where the membrane top layer shows defects so that no Knudsen diffusion characteristics are observed (as shown in Fig. 14), the dipping procedure can be repeated [49]. Defects can be repaired in this way. At the places where pinholes and defects are present, the support is hardly or not at all covered with the top layer. Therefore the resistance to liquid transport is much lower at the site of a pinhole or defect than at any other site where the top layer is present. During the next dipping procedure, water is sucked faster into the support at the pinhole site, due to this lower resistance. So the gel-layer growth is

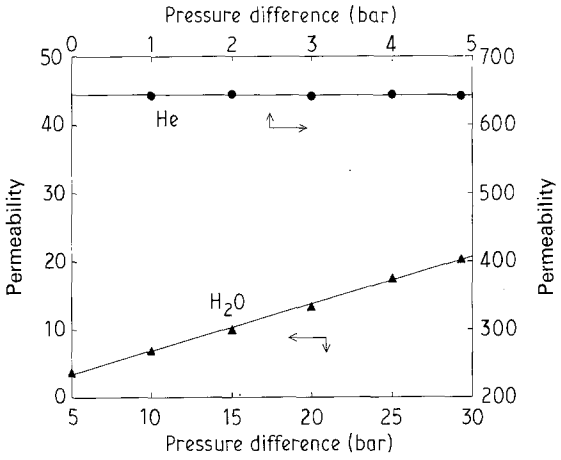

Figure 14 Helium and water permeabilities for titania membranes as a function of pressure difference across the membrane.

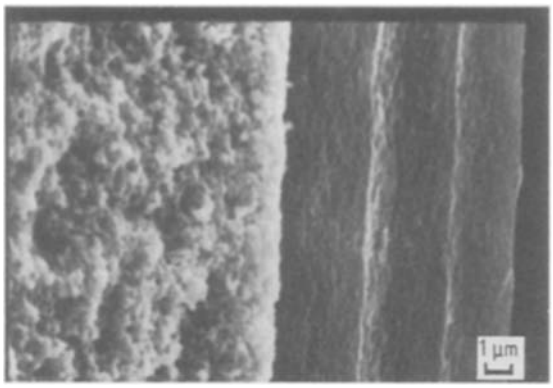

Figure 15 SEM photo of a supported titania membrane prepared after three successive film deposition procedures.

faster at the pinhole sites than at the rest of the surface. In this way pinholes and defects can be repaired.

Also, increased membrane thicknesses can be achieved by multiple (successive) dipping. As mentioned above, thin membranes are easier to process than thick membranes. By multiple dipping, crack-free titania membranes of more than 5 μm thickness could be prepared, as shown in Fig. 15, where the three successive layers can be distinguished. In a catalytically active membrane reactor, rather large membrane thicknesses can be important because the membrane thickness is directly related to the residence time of the reactants in the membrane and is an important process parameter for the membrane reactor performance. Finally, this technique can be used to prepare multilayer systems from different components (the so called 'sandwich' structures) with different catalytic properties, leading to the manufacture of bifunctional catalytic systems.

5. Conclusions

The synthesis and characterization of alumina and titania sols has been described. Alumina and titania sols may be prepared by a method in which a metal alkoxide is hydrolysed in excess of water and subsequently peptized with acid. Binary sols were prepared by mechanical mixing of alumina and titania sols. From these sols, alumina, titania and binary membranes may be prepared by a dipping process and according to the slip-casting mechanism. Mean pore diameters were obtained of 4.5 nm for TiO_2 membranes and 3 nm for Al_2O_3 membranes, with a narrow pore-size distribution. The porosities were 50 and 22% for the γ-Al_2O_3 and TiO_2 membranes, respectively.

The structural transformation of titania from the anatase to the rutile phase can be retarded by carrying out the hydrolysis of titanium tetra-isopropoxide in the presence of SO_4^{2-} ions. TiO_2 membranes were prepared which can be used up to 500 °C.

The introduction of organic additives in the dipping solution (e.g. PVA for alumina membranes, PVA and HPC for titania membranes) decreases the sensitivity of the membrane formation process for forming defects. The organic additives do not cause significant changes to the structures of the calcined membranes.

The titania membrane formation process has been optimized. Important factors determining the quality of the titania layers are the surface roughness of the support, and the layer thickness which must not exceed a value of 2 μm in a single process step.

Titania membranes have a lower tortuosity than do alumina membranes. This is in agreement with the difference in particle morphology between the plate-shaped alumina crystallites and the spherically-shaped titania crystallites.

By repeating the dipping procedure, possible defects in the membrane layer can be repaired. This technique can also be used for the preparation either of thick membrane layers or of multilayer membrane layers consisting of different components.

Acknowledgements

Philips N. V. Elcoma is thanked for supplying the α-alumina powder for the preparation of the supports. The financial asistance of the Dutch Innovative Program on Membrane Science (IOP-m) is gratefully appreciated.

References

1. H. K. LONSDALE, *J. Membr. Sci.* **10** (1985) 81.
2. H. STRATHMAN, *ibid.* **9** (1986) 121.
3. R. D. NOBLE, *Sep. Sci. Tech.* **22** (1987) 731.
4. E. K. LEE, *Encycl. Phys. Sci.* **8** (1987) 21.
5. S. L. MATSON, J. LOPEZ and J. A. QUINN, *Chem. Engng Sci.* **38** (1983) 503.
6. S. L. MATSON and J. A. QUINN, *Ann. N.Y. Acad. Sci.* **469** (1986) 152.
7. N. ITOH, Y. SHINDO, T. HAKUTA and H. YOSHITONE, *Int. J. Hydrogen Energy* **9** (1984) 835.
8. K. MOHAN and R. GOVIND, *Sep. Sci. Tech* **23** (1988) 1715.
9. K. MOHAN and R. GOVIND, *AIChE J.* **34** (1988) 1493.
10. O. SHINIJ, M. MISONO and Y. YONEDA, *Bull. Chem. Soc. Jpn* **55** (1982) 2760.
11. N. ITOH, *AIChE J.* **33** (1987) 1576.
12. J. N. ARMOR, *Appl. Catal.* **49** (1989) 1.
13. R. J. DELLEFIELD, presented at the AIChE Summer National Meeting, Denver Co., August 1988.
14. H. P. HSIEH, *AIChE Symp. Ser.* **84** (1988) 1.

15. H. J. SLOOT, PhD Thesis, I.S.B.N. 90–9004092–7, University of Twente, (1991).
16. A. S. MICHAELS, *Chem. Engng Prog.* **64** (1968) 31.
17. Catalytica study No. 4187 MR, "Catalytic membrane reactors: Concepts and Applications" (1988).
18. T. J. STANLEY and J. A. QUINN, *Chem. Engng Sci.* **42** (1987) 2313.
19. V. T. ZASPALIS, W. van PRAAG, K. KEIZER, J. G. van OMMEN, J. R. H. ROSS and A. J. BURGGRAAF, *Appl. Catal.* **74** (1991) 205.
20. J. G. A. BITTER, British Patent Application No. 8 629 135 (1986).
21. V. M. GRYAZNOV, *Zeits. Phys. Chem. Neue Folge* **147** (1986) 123.
22. D. E. MEGIRIS, in Proceedings of the 1st International Conference on Inorganic Membranes, edited by L. Cot, Montpellier, July 1989, p. 355.
23. R. J. R. UHLHORN, M. H. B. J. HUIS IN'T VELD, K. KEIZER and A. J. BURGGRAAF, in *ibid.* p. 323.
24. M. ASAEDA and L. D. DU, *J. Chem. Engng Jpn* **19** (1986) 84.
25. A. J. BURGGRAAF and K. KEIZER in "Inorganic Membranes: Synthesis Characteristics and Applications", edited by R. R. Bhave, (Van Nostrand Reinhold, New York, 1990) ch. 2.
26. J. CHARPIN, P. BERGEZ, F. VALIN, H. BARNIER, A. MAUREL and J. M. MARTINET, *Ind. Ceram.* **8** (1988) 23.
27. K. KEIZER and A. J. BURGGRAAF, *Sci. Ceram* **14** (1988) 83.
28. M. A. C. G. van de GRAAF, J. H. H. ter MAAT and A. J. BURGGRAAF, in "Ceramic Powders", edited by P. Vincenzini (Elsevier Scientific Publ. Coy., 1983), p. 783.
29. Y. KUROKAWA, T. SHIRAKAWA, S. SAITO and N. YUI, *J. Mater Sci. Lett.* **5** (1986) 1070.
30. E. J. WITZEMAN, *J. Amer. Chem. Soc.* **37** (1915) 1079.
31. A. F. M. LEENAARS, K. KEIZER and A. J. BURGGRAAF, *J. Mater Sci.*, **19** (1984) 1077.
32. A. LARBOT, J. A. ALARY, C. GUIZARD and L. COT, *Int. J. High Tech. Ceram* **3** (1987) 143.
33. B. E. YOLDAS, *J. Non-cryst. Solids* **51** (1982) 105.
34. R. J. van VUREN, B. C. BONEKAMP, K. KEIZER, R. J. R. UHLHORN, H. J. VERINGA and A. J. BURGGRAAF, in "High Tech Ceramics", edited by P. Vincenzini, (Elsevier, Amsterdam, 1987) p. 2235
35. A. F. M. LEENAARS and A. J. BURGGRAAF, *J. Coll. Interface Sci.* **105** (1985) 27.
36. J. L. WOODHEAD, UK Patent Application No. 14 12937 (1975).
37. B. E. YOLDAS, *J. Mater Sci.* **21** (1986) 1087.
38. B. E. YOLDAS, *J. Non-cryst. Solids* **51** (1982) 105.
39. V. T. ZASPALIS, K. KEIZER and A. J. BURGGRAAF, European Pattern Application No. 8901475 (1989).
40. J. L. WOODHEAD, *Sci. Ceram* **9** (1977) 29.
41. R. D. SHANNON, J. Appl. Phys. **35** (1964) 1964.
42. R. D. SHANNON and J. A. PASK, *J. Amer. Ceram. Soc.* **48** (1965) 391.
43. S. R. YOGONARASIMHAN and C. N. R. RAO, *Trans. Faraday Soc.* **58** (1962) 1579.
44. W. F. SULLIVAN and J. R. COLLEMAN, *J. Inorg. Nucl. Chem.* **24** (1962) 645.
45. K. J. D. MACKENZIE, *J. Brit. Chem. Soc.* **74** (1975) 121.
46. Y. IIDA and S. OZAKI, *J. Amer. Ceram. Soc.* **44** (1961) 3.
47. J. ZARZYCKI, in "Ultrastructure Processing of Ceramics", edited by L. L. Hench and P. R. Ulrich (Wiley, New York, 1984) 27.
48. L. L. HENCH, in "Science of Ceramic Chemical Processing", edited by L. L. Hench and P. R. Ulrich (Wiley, New York, 1986).
49. R. J. UHLHORN, PhD thesis, ISBN. 90–9003618–0, University of Twente (1990).
50. J. H. L. VONCKEN, K. P. KUMAR, K. KEIZER and A. J. BURGGRAAF, presented at the Materials Research Society Spring Meeting, Symposium H7.3, San Francisco, 1990.
51. G. W. SCHERER, *J. Non-Cryst. Solids* **87** (1986) 199.
52. *Iden, ibid.* **89** (1987) 217.
53. G. A. CROOPNICK and D. M. SCRUGGS, US Patent No. 4529 668 (1984).
54. J. N. ARMOR, European Patent Application No. 87303335.1 (1987).
55. J. E. KORESH, presented at the International Workshop on Membranes for Gas and Vapour Separation, Jerusalem, September 1988.
56. J. B. WACHTMAN and R. A. HABER, *Chem. Engng Prog.* 82(1) (1986) 39.
57. J. A. QUINN, W. S. ANDERSON, W. S. HO and W. PETZNY, *Biophys. J.* **12** (1972) 990.

Received 25 October 1990
and accepted 25 March 1991